

## Supporting Information for

# An efficient, robust new scheme for establishing broadband homonuclear correlations in biomolecular solid state NMR

Dr. Sungsool Wi<sup>1\*</sup> and Prof. Dr. Lucio Frydman<sup>1,2</sup>

<sup>1</sup> National High Magnetic Field Laboratory, Tallahassee, Florida 32304, USA

<sup>2</sup> Department of Chemical and Biological Physics, Weizmann Institute of Sciences, Rehovot, Israel

### 1. On the formation of harmonic AL FRESCO recoupling modes driven by the sampling of the chirped pulse.

Figures 2, 4 predict a strong periodicity in the offset differences which will be most efficiently recoupled by the AL FRESCO scheme. Eqs. (1)-(6) suggest that these optimal <sup>13</sup>C-<sup>13</sup>C polarization transfers will occur for offsets  $\Delta\Omega = \pm j|gv_r - l/\Delta t|$ ; the number of harmonic modes that will contribute to the method will be maximized by minimizing the  $|gv_r - l/\Delta t| \neq 0$  term with an appropriate  $g$  and  $l$  combination, for a given set of  $v_r$  and  $\Delta t$  values. If considering the cases shown in Figure 2 of the main text as an example, Table S1 summarizes the frequency positions (in ppm) of the harmonics predicted in this manner as a function of  $g$  and  $l$ . Shown in this table with a red font are the choices that maximize this offset-frequency dependent <sup>13</sup>C-<sup>13</sup>C signal transfer harmonics –even in the case of breaking the  $1/\Delta t > BW$  Nyquist criterion. Highlighted in red bold font, are the actual values evidenced by the simulations as most effective harmonics in the recoupling process.

**Table S1.** Calculation of  $|gv_r - l/\Delta t|/\nu_0(^{13}\text{C})$  using the  $v_r$  and  $\Delta t$  given in Figure 2.

$\Delta t = 5 \mu\text{s}$	$l = 1$	$l = 2$	$l = 3$	$l = 4$	$l = 5$
$g = 1$	933.3	2266.7	3600	4933.3	6266.7
$g = 2$	533.3	1866.7	3200	4533.3	5866.7
$g = 3$	<b>133.3</b>	1466.7	2800	4133.3	5466.7
$g = 4$	266.7	1066.7	2400	3733.3	5066.7
$g = 5$	666.7	666.7	2000	3333.3	4666.7
$g = 6$	1066.7	266.7	1600	2933.3	4266.7
$g = 7$	1466.7	<b>133.3</b>	1200	2533.3	3866.7
$g = 8$	1866.7	533.3	800	2133.3	3466.7
$g = 9$	2266.7	933.3	<b>400.0</b>	1733.3	3066.7
$g = 10$	2666.7	1333.3	0	1333.3	2666.7

$\Delta t = 10 \mu\text{s}$	$l = 1$	$l = 2$	$l = 3$	$l = 4$	$l = 5$
$g = 1$	266.7	<b>133.3</b>	533.3	933.3	1333
$g = 2$	933.3	533.3	<b>133.3</b>	266.7	666.7
$g = 3$	1600.	1200.	800.0	400.0	0
$g = 4$	2267	1867	1467	1067	666.7
$g = 5$	2933	2533	2133	1733	1333
$g = 6$	3600.	3200.	2800.	2400.	2000.
$g = 7$	4267	3867	3467	3067	2667
$g = 8$	4933	4533	4133	3733	3333
$g = 9$	5600.	5200.	4800.	4400.	4000.
$g = 10$	6267	5867	5467	5067	4667

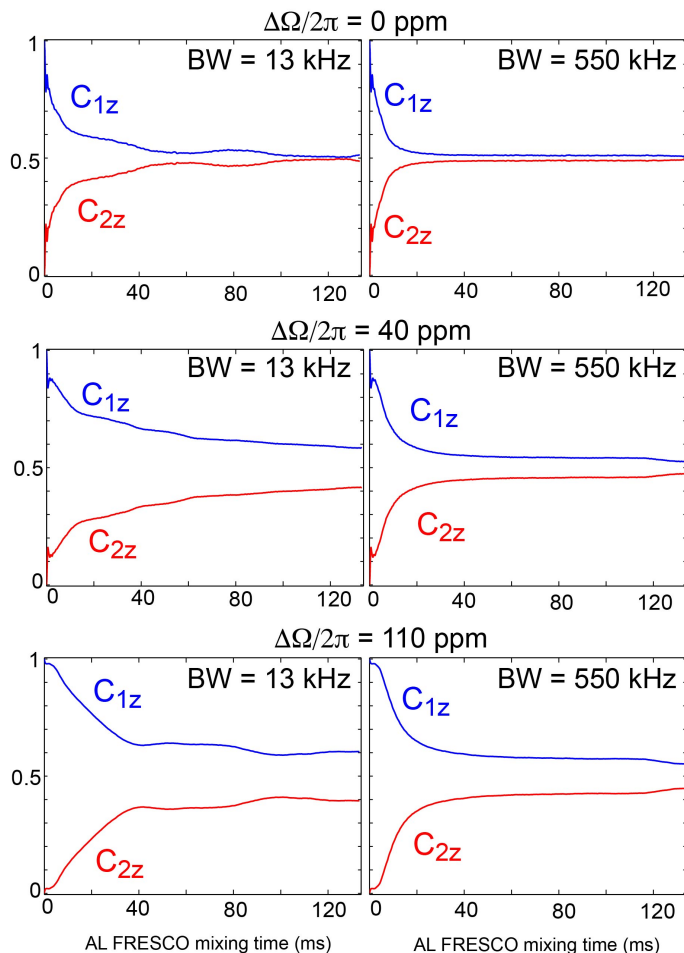
$\Delta t = 20 \mu\text{s}$	$l = 1$	$l = 2$	$l = 3$	$l = 4$	$l = 5$
$g = 1$	66.67	466.7	866.7	1267	1667
$g = 2$	266.7	133.3	533.3	933.3	1333
$g = 3$	600.0	200.0	200.0	600.0	1000.
$g = 4$	933.3	533.3	133.3	266.7	666.7
$g = 5$	1267	866.7	466.7	66.67	333.3
$g = 6$	1600.	1200.	800.0	400.0	0
$g = 7$	1933	1533	1133	733.3	333.3
$g = 8$	2267	1867	1467	1067	666.7
$g = 9$	2600.	2200.	1800.	1400.	1000.
$g = 10$	2933	2533	2133	1733	1333

$\Delta t = 60 \mu\text{s}$	$l = 1$	$l = 2$	$l = 3$	$l = 4$	$l = 5$
$g = 1$	288.9	688.9	1089	1489	1889
$g = 2$	177.8	577.8	977.8	1378	1778
$g = 3$	66.67	466.7	866.7	1267	1667
$g = 4$	44.44	355.6	755.6	1156	1556
$g = 5$	155.6	244.4	644.4	1044	1444
$g = 6$	266.7	133.3	533.3	933.3	1333
$g = 7$	377.8	22.22	422.2	822.2	1222
$g = 8$	488.9	88.89	311.1	711.1	1111
$g = 9$	600.0	200.0	200.0	600.0	1000.
$g = 18$	1600.	1200.	800.0	400.0	0

The unit of the numbers calculated in this table is in ppm.

Notice that when  $\Delta t = 5, 10, 20$  and  $60 \mu\text{s}$ , and for  $\nu_r = 60 \text{ kHz}$  and  $\nu_0(^{13}\text{C}) = 150 \text{ MHz}$ , the calculated  $|g\nu_r - l/\Delta t|/\nu_0(^{13}\text{C})$  basis for  $\Delta\Omega$  corresponds to 400 ppm ( $g = 9, l = 3$ ), 133.3 ppm ( $g = 1, l = 2$ ), 66.67 ppm ( $g = 1, l = 1$ ), and 22.22 ppm ( $g = 7, l = 2$ ), respectively. These values are highlighted in red in Table S1, and they match the gaps between adjacent harmonics observed in Figure 2. Notice that (i) even if there are multiple ( $g, l$ ) combinations that minimize the  $|g\nu_r - l/\Delta t|/\nu_0(^{13}\text{C})$  term, the combination that uses the smallest integers usually corresponds to the best recoupling condition; and (ii) even if  $\Delta t$  matches an integer multiple of the MAS rotational period so that the  $|g\nu_r - l/\Delta t|$  term becomes minimized or even zero, this synchronization does not necessarily provide the best overall recoupling results. AL FRESCO's  $\Delta t$  dependence is actually quite generous and those experimental spectra obtained with  $|g\nu_r - l/\Delta t| = 0$  condition are still in good qualities although it is not necessarily the best. Since this criterion is less significant as the MAS spinning rate decreases, when  $\Delta t = 4T_r$  or  $5T_r$ , for instance, at  $\nu_r = 12 \text{ kHz}$ , the spectral quality of a 2D  $^{13}\text{C}$ - $^{13}\text{C}$  correlation spectrum was excellent.

## 2. On the chirped pulse RF bandwidth (BW) and its sampling ( $\Delta t$ ).



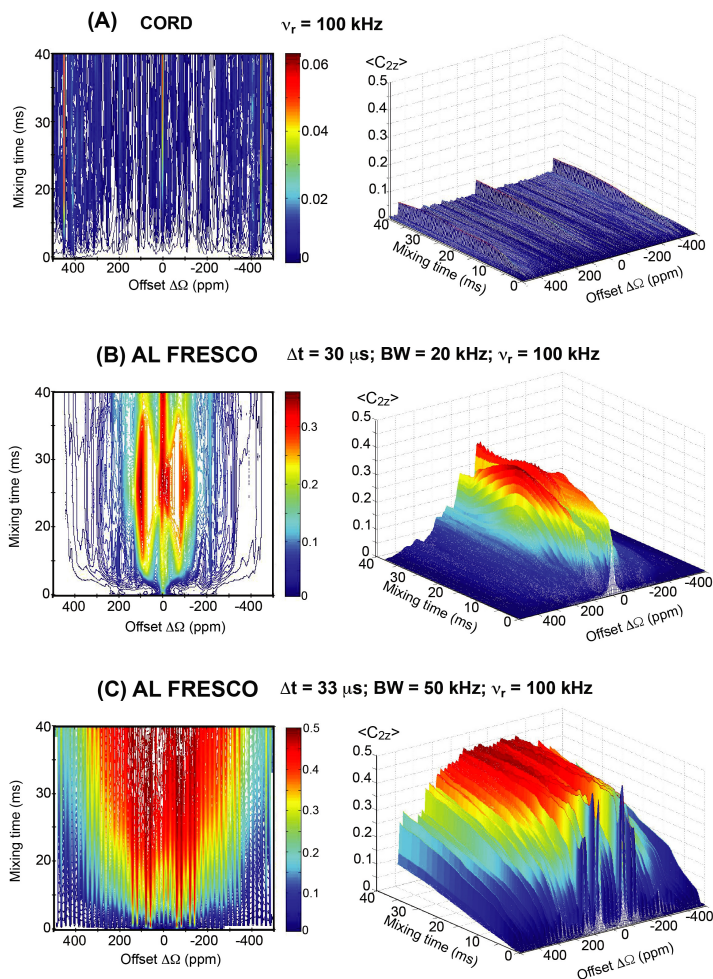
**Supporting Figure S1.** BW's influence on the AL FRESCO's mixing efficiency simulated on a  $H_1-C_1-C_2-H_2$  spin system (Fig. 2, main text) when its value changes vs  $1/\Delta t$ . For all cases  $\Delta t = 75 \mu s$  and the  $C_{1z} \rightarrow C_{2z}$  signal transfer ( $C_{1z} = 1$ ;  $C_{2z} = 0$  for  $\tau_{mix} = 0$ ) is calculated as a function of mixing time  $\tau_{mix}$ ,  $0 \leq \tau_{mix} \leq t_p = 133 ms$ . Notice the faster  $C_{1z} \rightarrow C_{2z}$  polarization transfers occurring when  $BW = 550 kHz$  for all  $\Delta\Omega$ . Sampling the pulse at a faster rate that satisfies the Nyquist criterion for all BWs, minimizes this efficiency.

It was observed experimentally that AL FRESCO yields an improved polarization transfer efficiency when the chirp pulse is set with a  $BW \geq 1/\Delta t$  undersampling condition. Supporting Figure S1 examines this feature, by showing  $C_{1z} \rightarrow C_{2z}$  polarization transfer efficiencies calculated on a  $H_1-C_1-C_2-H_2$  spin system (Figure 2, main text) as function of the BW value. The signal transfer curves were calculated for  $BW = 13 kHz$  ( $< 1/\Delta t$ ) and  $BW = 550 kHz$  ( $\gg 1/\Delta t$ ); in all cases for a pulse length  $t_p = 133 ms$ . These calculations were repeated three different  $\Delta\Omega$ s ( $\Delta\Omega/2\pi = 0 ppm$ ,  $40 ppm$  and  $110 ppm$ ) and for all three cases the transfer efficiency was better when BW was undersampled (see also the experimental spectra in Figure 7).

## 3. AL FRESCO at faster spinning rates

Supporting Figure S2 compares expectations of AL FRESCO and CORD mixing schemes, when assayed at  $\nu_r = 100 kHz$ . The  $C_{1z} \rightarrow C_{2z}$  signal transfer efficiency observed in the AL FRESCO simulation is still very efficient even under this ultrafast spinning case; it requires a weak RF field strength ( $\nu_{1H} = 15 kHz$ ) and is still very much affected by the  $\Delta t$  and BW values used as can be seen from (B) and (C). The case of  $\Delta t = 30 \mu s$  corresponds to the case where  $\Delta t$  is matched to  $3/\nu_r$ . In the case of  $\Delta t = 33 \mu s$ , where  $\Delta t$  is greater than  $3/\nu_r$  (BW

$= 50 \text{ kHz} \gg 1/\Delta t$ ), an excellent  $C_{1z} \rightarrow C_{2z}$  transfer is generated that is spanning over the whole offset frequency profile.

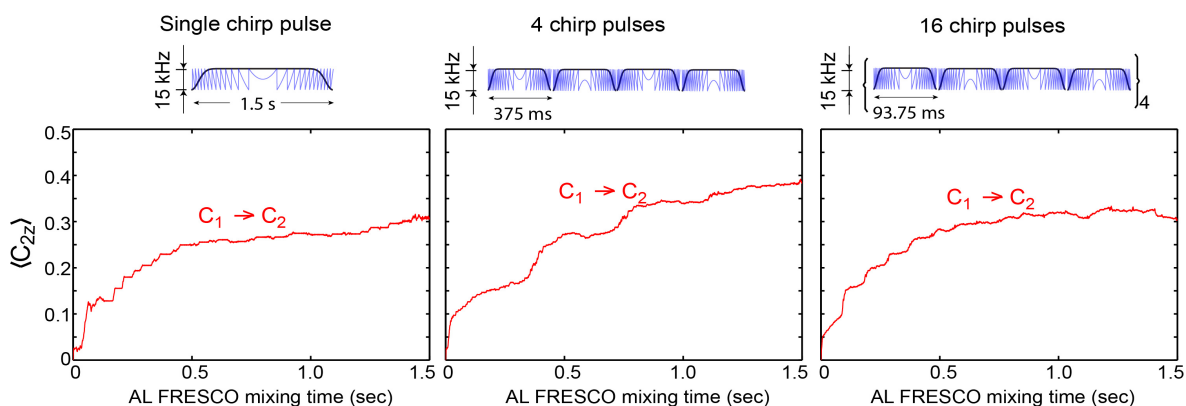


**Supporting Figure S2.** AL FRESKO and CORD efficiencies calculated for a MAS rate  $\nu_r = 100 \text{ kHz}$ . The RF pulse power used for the AL FRESKO scheme was  $\nu_{1H} = 15 \text{ kHz}$  (B and C), whereas CORD scheme 100 kHz for 13.3 ms and 50 kHz for 26.7 ms throughout its whole 40 ms mixing time (A). The spin system used in these simulations is as that assumed in Figure 4, and so were the range of offsets and AL FRESKO time evolution periods considered. Notice that although  $\nu_r = 100 \text{ kHz}$  the  $C_{1z} \rightarrow C_{2z}$  transfer efficiency observed in AL FRESKO is still as in the  $\nu_r = 60 \text{ kHz}$  case, whereas the CORD transfer is notably weakened. Notice as well how the  $C_{1z} \rightarrow C_{2z}$  AL FRESKO transfer efficiency is very much affected by the  $\Delta t$  and BW values used (B and C). The  $\Delta t = 30 \text{ }\mu\text{s}$  case (B) corresponds to  $\Delta t = 3/\nu_r$  leading to a broader rotational resonance condition around  $\Delta\Omega=0$ , whereas in the  $\Delta t = 33 \text{ }\mu\text{s}$  case (C) a good, broadband  $C_{1z} \rightarrow C_{2z}$  transfer spanning the whole offset frequency profile arises.

#### 4. Additional considerations pertaining AL FRESKO recoupling

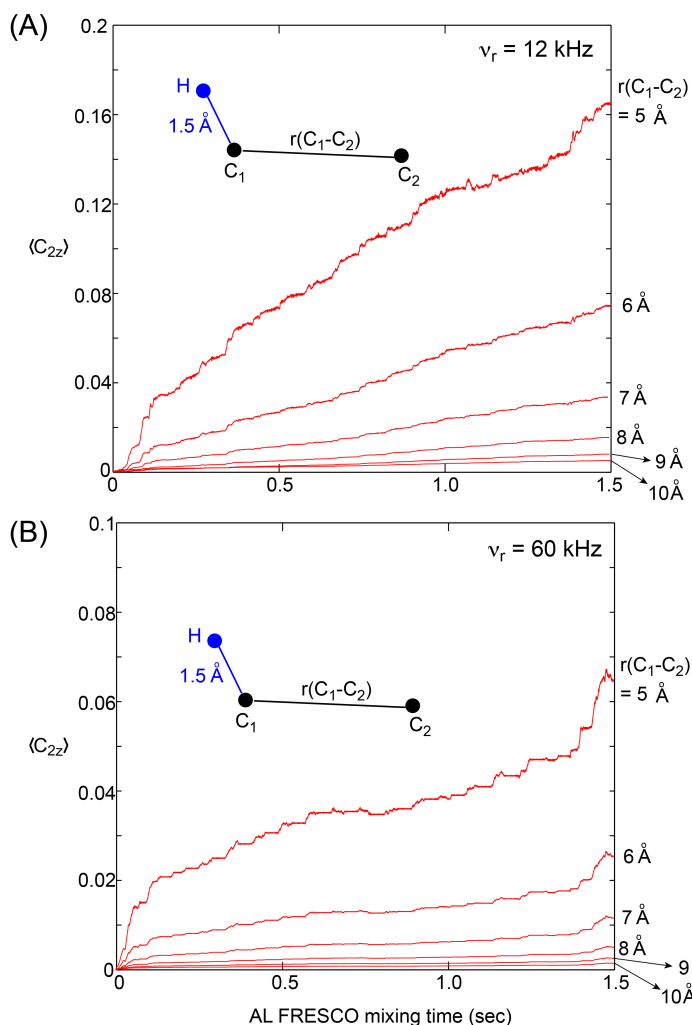
In this subsection we summarize various additional aspects of AL FRESKO mixing, as derived from numerical simulations on simple models.

The first consideration concerns the relative advantages of employing a single vs a train of multiple chirped pulses, for executing the mixing scheme. This is partly examined in Supporting Figure S3, which compares the results of using a single chirp pulse ( $\tau_{\text{mix}} = t_p = 1.5 \text{ s}$ ), a train of 4 chirped pulses ( $\tau_{\text{mix}} = 4t_p = 1.5 \text{ s}$ ;  $t_p = 375 \text{ ms}$ ), or 16 chirped pulses ( $\tau_{\text{mix}} = 16t_p = 1.5 \text{ s}$ ;  $t_p = 93.75 \text{ ms}$ )—always with  $\nu_{1H} = 15 \text{ kHz}$ ,  $\nu_r = 60 \text{ kHz}$ ,  $\Delta t = 75 \text{ }\mu\text{s}$  and  $\text{BW} = 250 \text{ kHz}$ . As can be seen from this Figure a train of multiple chirped pulses gives, overall, an improved efficiency—even if the same total mixing time length is used. It thus appears that, as the effects of several chirped pulses add up and accumulate, the overall efficiency of the mixing is improved at the end of the mixing. Interestingly however, at some point (e.g., 16 chirps) no further improvements are observed in the  $C_{1z} \rightarrow C_{2z}$  transfers—even if the initial buildup rate is improved.



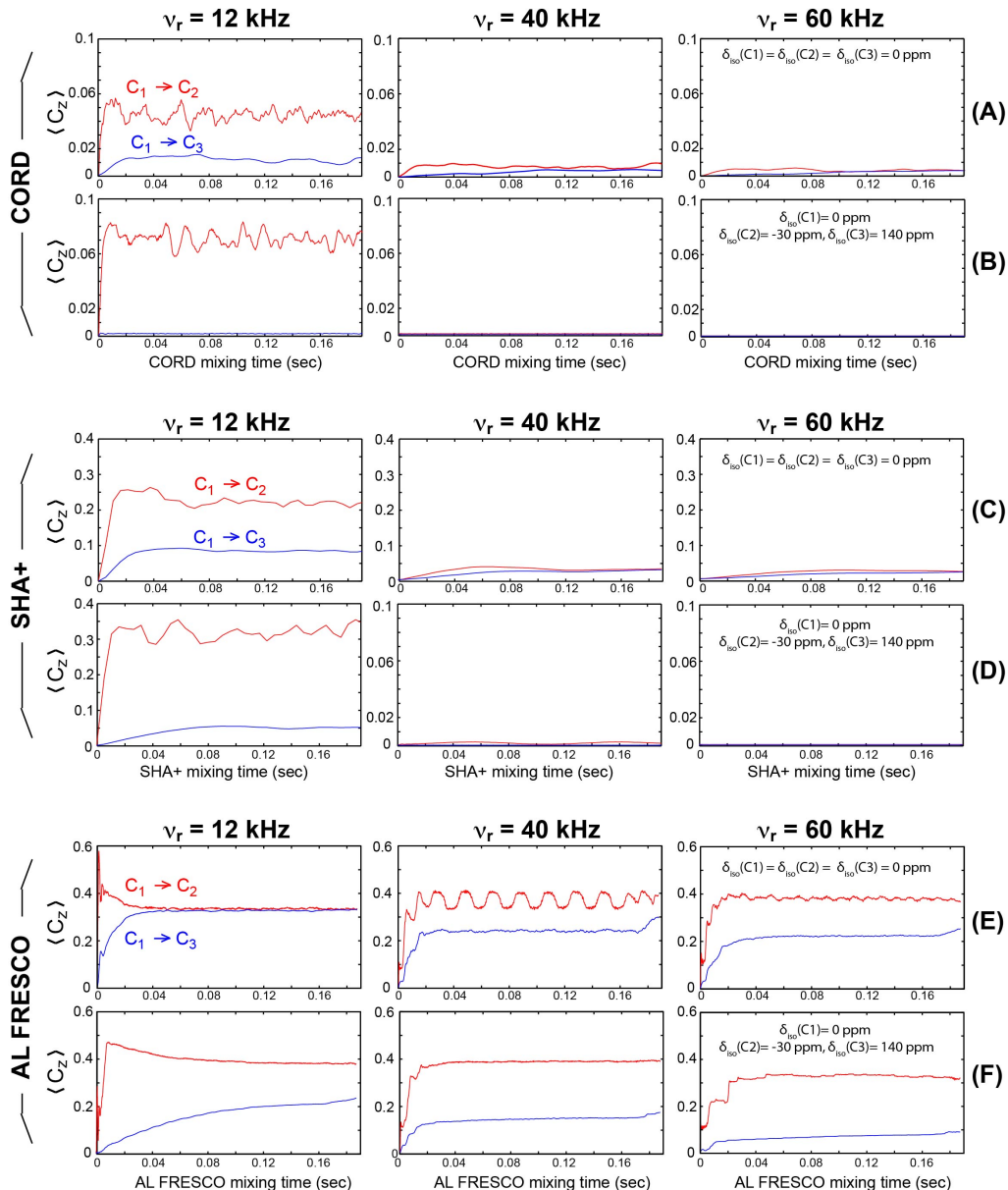
**Supporting Figure S3.** On the potential advantage of employing multiple chirped pulses. These simulations assumed a three-spin system, H-C<sub>1</sub>-C<sub>2</sub>, with  $r(\text{H-C}_1) = 1.5 \text{ \AA}$ ,  $r(\text{C}_1\text{-C}_2) = 3 \text{ \AA}$ ,  $\nu_r = 60 \text{ kHz}$ ,  $\Delta t = 75 \text{ \mu s}$ ,  $\text{BW} = 250 \text{ kHz}$  and  $\nu_0(^1\text{H}) = 600 \text{ MHz}$ . Coinciding dipolar vectors and chemical shift tensors were assumed for simplicity. The chemical shift parameters involved were:  $\delta_{iso}^{C_1} = 0 \text{ ppm}$ ,  $\delta_{CSA}^{C_1} = 40 \text{ ppm}$ ,  $\eta_{C_1} = 0.3$ ;  $\delta_{iso}^{C_2} = 20 \text{ ppm}$ ,  $\delta_{CSA}^{C_2} = 40 \text{ ppm}$ ,  $\eta_{C_2} = 0.2$ ;  $\delta_{iso}^H = 0 \text{ ppm}$ ,  $\delta_{CSA}^H = 2 \text{ ppm}$ ,  $\eta_{C_1} = 0.2$ . The mixing with 16 chirps provides a faster initial C<sub>1</sub> → C<sub>2</sub> signal transfer rate among all cases considered –but not the highest transfer. Note the stepwise build-up of the polarization transfer at the start of each chirp unit in the train.

Another consideration worth tackling concerns estimating what kind of maximal <sup>13</sup>C-<sup>13</sup>C distances can the AL FRESKO mixing scheme establish. Of course, this must be proved experimentally on a real sample system involving multiple nuclides and constrained signal-to-noise. But a rough idea of this limit can be assessed by assuming a simple system (e.g., <sup>1</sup>H-<sup>13</sup>C<sub>1</sub>-<sup>13</sup>C<sub>2</sub>) and calculating what cross-peak intensities can be expected for the C<sub>1</sub>-C<sub>2</sub> pair under a long mixing time (e.g.,  $\tau_{\text{mix}} = 1.5 \text{ s}$ ). Supporting Figure S4 calculates this for various <sup>13</sup>C<sub>1</sub>-<sup>13</sup>C<sub>2</sub> distances in the 5~10 Å range ( $r[^1\text{H-}^{13}\text{C}_1] = 1.5 \text{ \AA}$ ), upon applying 16 <sup>1</sup>H chirped pulses ( $t_p = 93.75 \text{ ms}$ ) with  $\nu_{1\text{H}} = 15 \text{ kHz}$ , and for MAS rates  $\nu_r = 12$  and 60 kHz. Since only a <sup>13</sup>C-<sup>13</sup>C pair is considered no potential dipolar truncation effects are possible (although these should be relatively small), as aren't signal transfers in a relayed fashion. In any case, particularly at the case of  $\nu_r = 12 \text{ kHz}$ , it appears that distances of up to 8 Å should give origin to detectable cross-peaks. Still, in real systems, some of this polarization transfer may arise as a result of relayed transfers; Figure S6 and its associated discussion consider this possibility in greater detail.



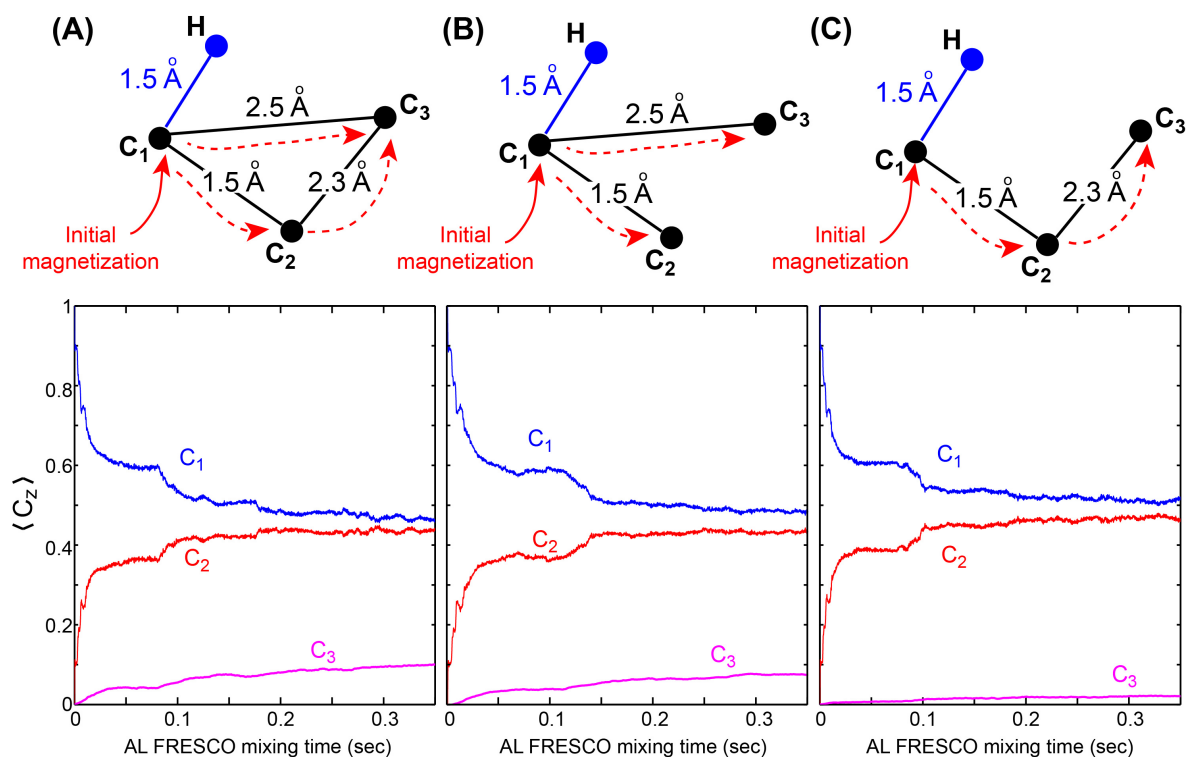
**Supporting Figure S4.** AL FRESKO's long-distance mixing capabilities, simulated on a  $^1\text{H}-\text{C}_1-\text{C}_2$  spin system. A variable  $^{13}\text{C}_1-^{13}\text{C}_2$  spin pair distance was assumed (with a fixed  $\text{H}-^{13}\text{C}_1$   $1.5 \text{ \AA}$  distance), as were two MAS rates ( $\nu_r = 12, 60$  kHz). Other coupling tensor parameters were as in Fig. S3. Mixing proceeded over a  $\tau_{\text{mix}} = 1.5$  s time and involved 16 chirped pulses, each of duration  $t_p = 93.75$  ms.. Additional chirped pulse parameters were  $\Delta t = 75 \mu\text{s}$ ;  $\text{BW} = 250$  kHz;  $\nu_{1\text{H}} = 15$  kHz.

It is also worth comparing the performance of AL FRESKO's mixing scheme with that of existing methods such as CORD<sup>2,3</sup> and SHA<sup>4-6</sup>, that can also lead to efficient  $^{13}\text{C}-^{13}\text{C}$  correlations –particularly when fast MAS rates are used. Supporting Figure S5 compares the  $^{13}\text{C}-^{13}\text{C}$  signals' build-up predicted for AL FRESKO, CORD and SHA+ mixing schemes, as calculated for a four-spin system  $\text{H}-\text{C}_1-\text{C}_2-\text{C}_3$ . Three different MAS rates ( $\nu_r = 12, 40, 60$  kHz) and two different chemical shift offsets were assumed: in one isotropic chemical shifts coincided for all carbons ( $\delta_{\text{CSA}}^{\text{C}_1} = 40$  ppm,  $\eta_{\text{C}_1} = 0$ ;  $\delta_{\text{CSA}}^{\text{C}_2} = 40$  ppm,  $\eta_{\text{C}_2} = 0.3$ ;  $\delta_{\text{CSA}}^{\text{C}_3} = 30$  ppm,  $\eta_{\text{C}_3} = 0.2$ ) (A, C, E), and in the other three different isotropic chemical shifts ( $\delta_{\text{iso}}^{\text{C}_1} = 0$  ppm,  $\delta_{\text{iso}}^{\text{C}_2} = -30$  ppm,  $\delta_{\text{iso}}^{\text{C}_3} = 140$  ppm; B, D, F respectively) were considered –while keeping the same CSA tensor parameters. The chemical shift parameters considered for the proton were  $\delta_{\text{iso}}^{\text{H}} = 0$  ppm,  $\delta_{\text{CSA}}^{\text{H}} = 2$  ppm,  $\eta_{\text{H}} = 0.2$  ( $\nu_0[^1\text{H}] = 600$  MHz). For all cases, the AL FRESKO scheme shows a dramatic improvement in the signal build-ups of both  $\text{C}_2$  and  $\text{C}_3$ . AL FRESKO's advantages are particularly evident for the latter, most relevant case, involving the off-resonance sites subject to high MAS rate.



**Supporting Figure S5.** Comparing the AL FRESCO, CORD, and SHA+ performances at different MAS rates (12, 40, 60 kHz). A four-spin H-C<sub>1</sub>-C<sub>2</sub>-C<sub>3</sub> system was considered with internuclear distances  $r(\text{H-C}_1) = 1.5$ ,  $r(\text{C}_1\text{-C}_2) = 1.5$ , and  $r(\text{C}_1\text{-C}_3) = 2.5$  Å; no H-C<sub>2</sub>, H-C<sub>3</sub> or C<sub>2</sub>-C<sub>3</sub> couplings were considered (as in Fig. S6b). For each sequence two cases with different isotropic chemical shifts were considered: (Top of each experiment) Identically null isotropic shifts for all carbons ( $\delta_{CSA}^{C1} = 40$  ppm,  $\eta_{C1} = 0$ ;  $\delta_{CSA}^{C2} = 40$  ppm,  $\eta_{C2} = 0.3$ ;  $\delta_{CSA}^{C3} = 30$  ppm,  $\eta_{C3} = 0.2$ ) (A, C, E); (Bottom of each experiment) Three different chemical shifts –  $\delta_{iso}^{C1} = 0$  ppm,  $\delta_{iso}^{C2} = -30$  ppm, and  $\delta_{iso}^{C3} = 140$  ppm (B, D, F), with the CSA and  $\eta$  values same as above. The chemical shift parameters for the <sup>1</sup>H were  $\delta_{iso}^H = 0$  ppm,  $\delta_{CSA}^H = 2$  ppm,  $\eta_H = 0.2$  ( $\nu_0[{}^1\text{H}] = 600$  MHz). Coinciding dipolar vector and CSA tensor are assumed for each case. The mixing time employed for each case was  $\approx 190$  ms. Only a single chirp pulse of was used for the AL FRESCO mixing with  $\Delta t = 75$   $\mu\text{s}$ ,  $\text{BW} = 250$  kHz. Notice (i) the different vertical scales of the transfers, reflecting each sequence's efficiency; (ii) the benefits of AL FRESCO –particularly when dealing with a broad chemical shift range.

The last simulation discussed concerns AL FRESCO's magnetization relay behavior; i.e., the possibility that cross peaks between carbon sites  $C_1$  and  $C_3$  might appear due to a stepwise  $C_{1z} \rightarrow C_{2z} \rightarrow C_{3z}$  propagation. Again, a four-spin system H- $C_1$ - $C_2$ - $C_3$  was employed in this study, using geometry and parameters identical to those in Supporting Figure S5. Three different types of spin clusters were considered in Fig. S6: (A) one with all  $^{13}\text{C}$ - $^{13}\text{C}$  dipolar couplings active; (B) one with only  $C_1$ - $C_2$  and  $C_1$ - $C_3$  dipolar couplings considered (i.e., with admitting a direct  $C_1 \rightarrow C_3$  transfer); (C) one with only the  $C_1$ - $C_2$  and the  $C_2$ - $C_3$  couplings considered, so as to allow for the possibility of a relayed polarization transfer. As can be seen from Figure S6, the chances of  $C_1 \rightarrow C_3$  propagation via a relayed fashion is small – but not zero. Indeed, if comparing the steady state  $C_3$  signal received in all three cases, it is clear that there is a contribution arising from a  $C_{1z} \rightarrow C_{2z} \rightarrow C_{3z}$  relayed transfer: either by subtracting  $C_3$ (steady state) in (A) from (B) or by considering  $C_3$ (steady state) in (C), one can conclude that ca. 20% of what is observed as  $C_{1z} \rightarrow C_{3z}$  transmission is actually relayed by  $C_2$ . Naturally, the exact amount of relayed magnetization will depend on the geometry, offsets, anisotropies and recoupling conditions; still, Figure S6 gives a realistic appraisal of this phenomenon –which also arises in most DARR- and MIRROR-derived sequences.



**Supporting Figure S6.** Estimating relayed polarization transfer in AL FRESCO. All tensor and recoupling parameters were as in Supporting Figure S5B, and the transfer patterns considered for each case were as illustrated in the cartoons on top.  $C_{1z}=1$  magnetization was initially assumed, and the  $C_{2z}, C_{3z}$  buildups were monitored as function of mixing time. A train of 4 chirps was used in the mixing scheme ( $4t_p = 375$  ms;  $t_p = 93.75$  ms; only the 0~350 ms portion was shown in the figure). Chirp pulse parameters are:  $\Delta t = 75$   $\mu\text{s}$ ; BW = 250 kHz. The MAS rate was  $\nu_r = 60$  kHz.



#### 4. References:

- (1) Scholz, I.; Huber, M.; Manolikas, T.; Meier, B. H.; Ernst, M. *Chem. Phys. Lett.* **2008**, *460*, 278.
- (2) Hou, G.; Sun, S.; Han, Y.; Byeon, I.-J.; Ahn, J.; Concel, J.; Samoson, A.; Gronenborn, A. M.; Polenova, T. *J. Am. Chem. Soc.* **2011**, *133*, 3943.
- (3) Hou, G.; Yan, S.; Trébosc, J.; Amoureux, J.-P.; Polenova, T. *J. Magn. Reson.* **2013**, *232*, 18.
- (4) Hu, B.; Trébosc, J.; Lafon, O.; Chen, Q.; Masuda, Y.; Takegoshi, K.; Amoureux, J.-P. *ChemPhysChem* **2012**, *13*, 3585.
- (5) Shen, M.; Liu, Q.; Trébosc, J.; Lafon, O.; Masuda, Y.; Takegoshi, K.; Amoureux, J.-P.; Hu, B.; Chen, Q. *Solid State Nucl. Magn. Reson.* **2013**, *55-56*, 42.
- (6) Yan, X. J.; Hu, B. *Chinese J. Magn. Reson.* **2016**, *33*, 361.